

Scheme I

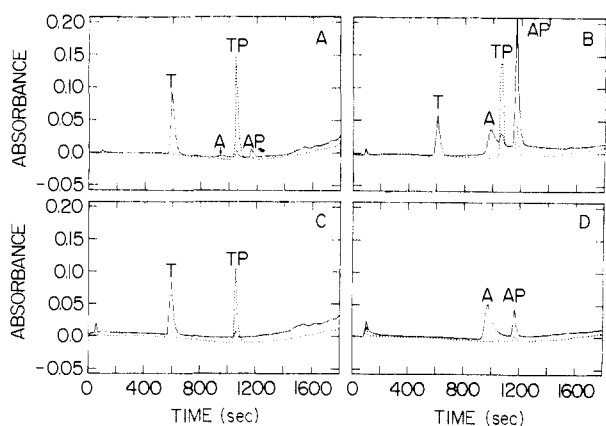
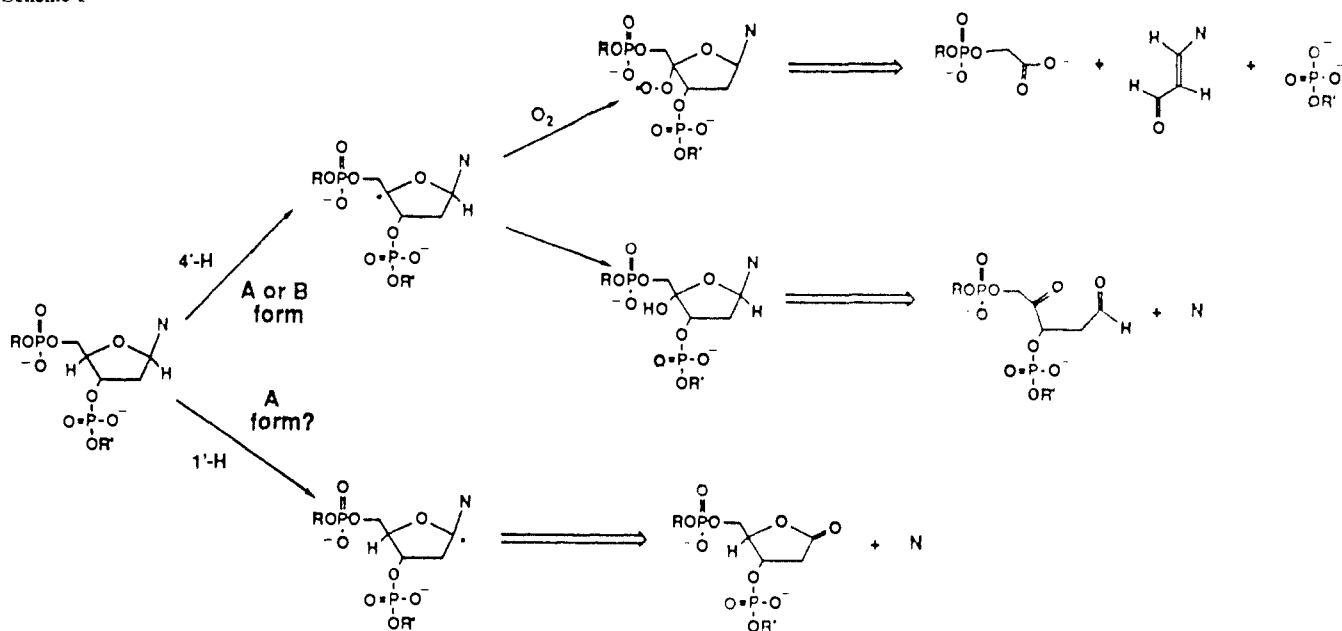


Figure 1. Reverse phase HPLC profiles for reactions of Fe(II)-bleomycin with A, poly(dA-dT); B, poly(dA)·poly(dT); C, poly(rA)·poly(dT); and D, poly(dA)·poly(rU). Solid lines and broken lines represent the UV absorbance at 260 and 300 nm, respectively: A = adenine; AP = adenine propenal; T = thymine; TP = thymine propenal.

of free base (Scheme I). Thus, the product ratio of poly(dA)·poly(rU) could be explained by an initial partitioning between 4'-hydrogen and 1'-hydrogen abstraction.¹³ It is particularly significant that the product ratio for poly(rA)·poly(dT) is similar to those found for the B-form DNAs. This hybrid is believed to be a B-form.^{6a,14}

While this hypothesis is speculative, it does suggest that bleomycin may serve as a useful probe of nucleic acid structure and may explain the observation by others of an apparent O_2 -independent release of free base by using heterogeneous DNA.^{4e} Our recent preliminary studies indicate that a significant portion of adenine release from poly(dA)·poly(rU) is insensitive to high O_2 concentrations as compared to the other duplexes, an observation consistent with 1'-hydrogen abstraction. Application of

the isotopic analyses developed by us to these hybrids should be informative and are in progress.

Acknowledgment. This work was supported by a grant from the National Institutes of Health (GM 34454).

Electrochemistry at the Water/Air Interface. Lateral Electron Transport in Langmuir Monolayers

Cindra A. Widrig, Cary J. Miller, and Marcin Majda*

Department of Chemistry
University of California, Berkeley
Berkeley, California 94720

Received November 6, 1987

Revised Manuscript Received January 15, 1988

In our recent reports, we have described electrochemical measurements of the lateral charge transport in self-assembled bilayers of electrochemically active amphiphiles.¹⁻³ In those measurements, a microporous aluminum oxide template was used to assemble bilayers composed of octadecyltrichlorosilane and an octadecyl derivative of naphthoquinone, ferrocene, or methylviologen. In all three systems, the lateral charge transport is sustained by the translational diffusion of the electroactive amphiphiles along the bilayer. In this communication, we report the results of the electrochemical measurements of lateral electron transport in amphiphilic monolayers spread at the water/air interface under controlled surface pressure conditions. In these experiments, a microelectrode is oriented *perpendicular* to the water/air interface and addresses an electroactive surfactant monolayer at that interface. In a system involving ferrocenylmethyl-dimethyloctadecylammonium perchlorate ($C_{18}Fc-ClO_4$) monolayer spread at the water/air interface, the electron transport occurs via lateral electron hopping in the monolayer.

The crucial part of the experiment involves the construction of a microelectrode and its positioning at the water/air interface. The microelectrodes are prepared by vapor-deposition of a 300 Å gold film at an ca. $1 \times 2 \text{ cm}^2$ glass slide. The surface of the gold film is then insulated and rendered hydrophobic by spin-coating an approximately 2000 Å thick layer of polystyrene. By

(13) A similar partitioning has been proposed for the nuclease activity of 1,10-phenanthrolinecopper(I) ion with DNA although the products differ from the bleomycin reaction: Goynes, T. E.; Sigman, D. S. *J. Am. Chem. Soc.* **1987**, *109*, 2846–2848.

(14) (a) Zimmerman, S. B.; Pfeiffer, B. H. *Proc. Natl. Acad. Sci. U.S.A.* **1981**, *78*, 78–82. (b) Gupta, G.; Sarma, M. H.; Sarma, R. H. *J. Mol. Biol.* **1985**, *186*, 463–469. (c) Krueger, W. C.; Li, L. H.; Moscovitz, A.; Prairie, M. D.; Petzold, G.; Swenson, D. H. *Biopolymers* **1985**, *24*, 1549–1572.

(1) Miller, C. J.; Majda, M. *J. Am. Chem. Soc.* **1986**, *108*, 3118.

(2) Miller, C. J.; Widrig, C. A.; Charych, D. H.; Majda, M. *J. Phys. Chem.*, in press.

(3) Goss, C. A.; Miller, C. J.; Majda, M. *J. Phys. Chem.*, in press.

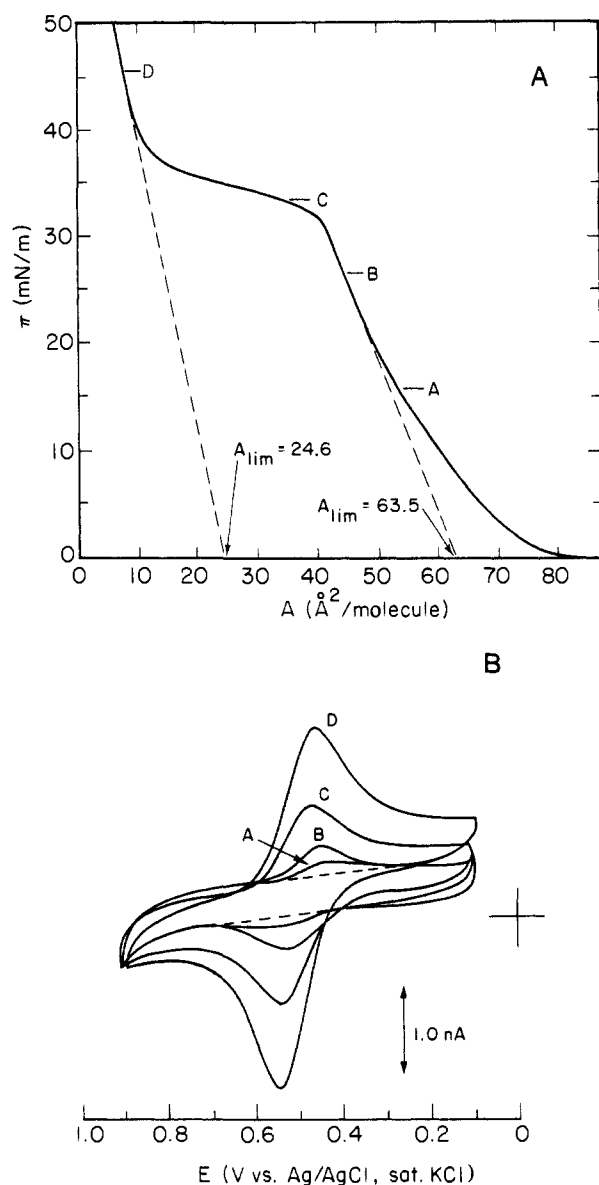


Figure 1. (A) A surface pressure versus area per molecule diagram for the compression of a $C_{18}Fc-ClO_4$ monolayer at the water (0.1 M $NaClO_4$)/air interface: $T = 23^\circ C$. The letter marks refer to the voltammograms in (B). (B) Selected cyclic voltammograms of $C_{18}Fc-ClO_4$ in the monolayer at the water/air interface corresponding with the points marked along the surface pressures versus area isotherm in (A); the dashed line background curve was recorded before spreading the monolayer: $v = 200$ mV/s.

scoring the back of the gold/polystyrene coated glass slide with a diamond pencil and breaking it into two 1 cm^2 pieces one obtains two microelectrodes. Each of them consists of an approximately 1 cm long, 300 \AA wide band of gold sandwiched between a hydrophilic glass substrate and a hydrophobic polystyrene layer.⁴ When a gold/polystyrene-coated glass slide is floating on the water surface with the gold/polystyrene layer facing upwards, the surface of water is brought in contact with the gold band microelectrode since water cannot wet the polystyrene layer. After recording the background current, a surfactant monolayer is spread at the water surface. During compression of a monolayer, surface pressure versus area isotherms and cyclic voltammograms can be recorded simultaneously.

Figure 1 shows a typical surface pressure versus area per molecule isotherm and a series of cyclic voltammograms recorded at various surface pressures for a monolayer of $C_{18}Fc-ClO_4$ spread

on $0.1\text{ M } NaClO_4$ subphase. The limiting area per molecule corresponding to the first rising portion of the isotherm depends on the time of equilibration of the system at $\pi = 0$ before the compression of the monolayer. It decreases from approximately 83 to 53 \AA^2 as the incubation time increases from 0 to 2 h. Facci and co-workers have reported a limiting area of 51 \AA^2 for the PF_6^- salt of the same surfactant spread on $0.1\text{ M } Na_2SO_4$ subphase and characterized it as consistent with the size of a ferrocene molecule.⁵ In our experiment, a transition is observed at ca. 30 mN/m which is followed by a second sharply rising segment of the isotherm (see Figure 1A). The extrapolation of the latter gives a limiting area of $24.2 \pm 1.4\text{ \AA}^2$ (average of 25 trials) which is independent of the equilibration time at the beginning of the experiment.

The recording of $\pi - A$ isotherms was accompanied by continuous cyclic voltammetric scanning at 200 mV/s . Figure 1B shows four selected voltammograms recorded at the points marked along the isotherm in Figure 1A. All cyclic voltammograms have the shape characteristic for a reversible, one-electron redox couple under semi-infinite diffusion controlled conditions. It is apparent that the ferrocene/ferrocenium redox couple preserves its reversibility in the compressed monolayer. Our system consisting of a one-dimensional electrode in a two-dimensional medium is analogous to a system of a planar, two-dimensional electrode in an electrolyte solution in that the former can be derived from the latter by the reduction of dimensionality of both the electrode and the medium. In this context, the shape of the voltammograms in Figure 1B is not unexpected.

The most interesting results are the following two features of the voltammetric behavior of this system. The first is the complete lack of electroactivity of the system below 15 mN/m . This suggests crystallization of the $C_{18}Fc-ClO_4$ molecules since otherwise we would expect to observe electroactivity limited by the translational diffusion of molecules to the electrode surface. The postulated crystallization of $C_{18}Fc-ClO_4$ is consistent with the time dependence of the limiting area per molecule for the first rising segment of the isotherm mentioned above. The second interesting feature of the voltammetric behavior is the increase of the peak current in the region B-C.⁶ This increase is significantly faster than could be expected from the increase of the surface concentration of the ferrocene surfactant. This behavior could correspond to coalescence of the individual crystallites which opens electron transport channels to an increasing fraction of the ferrocene centers. We could also postulate that the observed current increase is related to a change of distance and/or orientation between individual ferrocene moieties which increases the rate of electron self-exchange. The value of the second limiting area per molecule of 24.2 \AA^2 could be interpreted as a perpendicular offset of half of the ferrocene groups in the monolayer at high compression. In either case, the observed behavior provides a strong indication that the mechanism of the lateral electron propagation is electron hopping and not translational diffusion of the individual ferrocene surfactant molecules. In phospholipid monolayer films spread on a Langmuir-Blodgett trough, Peters and Beck observed decreasing translational diffusion coefficients with increasing surface pressure by using a fluorescence microphotolysis method.⁷ The second increase of the peak current in the region of the final rapid pressure increase in Figure 1A is consistent with the observed increase of the surface concentration of $C_{18}Fc-ClO_4$ in the compressed monolayer.

If we assume that all ferrocene centers are electroactive at point C along the isotherm, then the magnitude of the corresponding voltammetric peak current can be used to calculate the diffusion coefficient of electron hopping, D . By using the equation for the voltammetric peak current,⁸ one obtains from the data in Figure

(5) Facci, J. S.; Falcigno, P. A.; Gold, J. M. *Langmuir* **1986**, *2*, 732.

(6) Cyclic voltammograms recorded in the region A-B on the isotherm in Figure 2A exhibit small fluctuating current (appearing and disappearing) in the course of the compression of the monolayer.

(7) Peters, R.; Beck, K. *Proc. Natl. Acad. Sci. U.S.A.* **1983**, *80*, 7183.

(8) Bard, A. J.; Faulkner, L. R. *Electrochemical Methods; Fundamentals and Applications*; J. Wiley: New York, 1980; Chapter 6, p 218.

(4) An electrical contact is made by removing a small section of the polystyrene film in the middle of the glass slide and attaching a thin Pt wire to the gold surface with silver epoxy.

2 (curve C) $D = 4 \times 10^{-10}$ cm²/s. This corresponds, according to the Dahms–Ruff equation,^{9,10} to the rate constant of the electron exchange of ca. 2×10^4 M⁻¹ s⁻¹. The latter is two orders of magnitude smaller than a value obtained for a homogeneous solution.¹¹

$$D = \frac{\pi}{4} k_{\text{ex}} \delta^2 C \quad (1)$$

The results presented here are the first measurements of the lateral electron transport directly at the water/air interface under controlled surface pressure. It is easy to envision the relevance of these two-dimensional electrochemical experiments to the studies of the dynamics of lateral transport in organized monolayers and, in general, to the investigations of transport processes in biological membrane systems. Perhaps more importantly, the technique described here opens a possibility to investigate electron-transfer kinetics in well organized monolayer assemblies where the transfer of an electron involves molecules at known distances and in well defined and controllable orientations.

Acknowledgment. We gratefully acknowledge the National Science Foundation for supporting this research under Grant CHE-8504368.

(9) Dahms, H. J. *Phys. Chem.* **1968**, *72*, 362.

(10) Ruff, I.; Friedrich, V. J.; Demeter, K.; Csillag, K. *J. Phys. Chem.* **1971**, *75*, 3303.

(11) Yang, E. S.; Chan, M.-S.; Wahl, A. C. *J. Phys. Chem.* **1980**, *84*, 3094.

Actinide Bis(porphyrinate) π -Radical Cations and Dications, Including the X-ray Crystal Structure of $[(\text{TPP})_2\text{Th}][\text{SbCl}_6]$

Gregory S. Girolami,* Stanley N. Milam, and Kenneth S. Suslick*

School of Chemical Sciences
University of Illinois at Urbana–Champaign
505 S. Mathews Avenue
Urbana, Illinois 61801

Received November 19, 1987

The chemistry of actinide porphyrin complexes remains in large part undeveloped.^{1–3} We report here the first synthesis, isolation, and detailed characterization of several actinide bis-porphyrin sandwich complexes, including the neutral, π -radical monocation, and π -radical dication complexes,⁴ $[(\text{TPP})_2\text{M}]^{n+}$, where M = Th(IV) or U(IV) and $n = 0, 1$, or 2. In addition, the X-ray crystal structures of both the neutral Th complex and its oxidized π -radical cation, $[(\text{TPP})_2\text{Th}][\text{SbCl}_6]$, have been solved. These complexes are among the very first π -radical cations where close interaction between two porphyrins occurs. Moreover, these complexes belong to an unusual class of actinide complexes where redox processes can occur in near proximity to the f-element. In addition, the involvement of porphyrin π -radical cations is well established in a variety of biological processes, including the storage of oxidizing equivalents in the hydroperoxidases,⁵ the oxidation of hydrocarbons by cytochrome P450,⁶ and the generation of chemical potential in the photosynthetic reaction center.^{7,8}

(1) Girolami, G. S.; Milam, S. N.; Suslick, K. S. *Inorg. Chem.* **1987**, *26*, 343–344.

(2) (a) Dormond, A.; Belkalem, B.; Charpin, P.; Lance, M.; Vigner, D.; Folcher, G.; Guillard, R. *Inorg. Chem.* **1986**, *25*, 4785–4790. (b) Dormond, A.; Belkalem, B.; Guillard, R. *Polyhedron* **1984**, *1*, 107–112.

(3) Wong, C.-P.; Horrocks, W. D. *Tetrahedron Lett.* **1975**, *31*, 2637–2640.

(4) Abbreviations used: TPP = 5,10,15,20-tetraphenylporphyrinate, OEP = octaethylporphyrinate, thf = tetrahydrofuran, acac = 2,4-pentanedionate.

(5) Hewson, W. D.; Hager, L. P. *The Porphyrins*; Dolphin, D., Ed.; Academic Press: New York, 1979; Vol. 7, pp 295–332.

(6) *Cytochrome P450*; Ortiz de Montellano, P. R., Ed.; Plenum: New York, 1986.

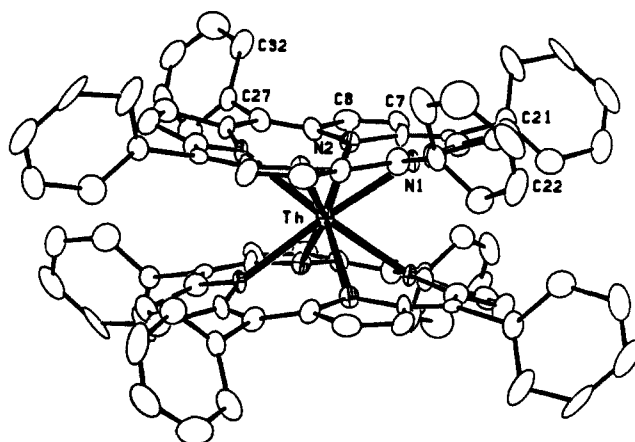


Figure 1. Molecular structure of the $[(\text{TPP})_2\text{Th}]^+$ cation. The Th–N average bond distance is 2.52 (2) Å; the distance between mean porphyrin planes is 2.89 Å with a twist angle of 31°.

We have recently described the preparation of the “sandwich” compound $(\text{TPP})_2\text{U}$ from $\text{U}(\text{NEt}_2)_4$ and H_2TPP in toluene¹ and find that the thorium analogue,⁹ $(\text{TPP})_2\text{Th}$, may be obtained in a similar manner from $\text{Th}(\text{NEt}_2)_4$.¹⁰ Cyclic voltammetry experiments in CHCl_3 reveal that both $(\text{TPP})_2\text{M}$ compounds undergo two chemically reversible oxidation processes near 580 and 990 mV versus SCE. The similarities of the cyclic voltammograms for the thorium and uranium complexes strongly suggest that both oxidations are porphyrin based.¹¹

The oxidized $[(\text{TPP})_2\text{M}]^+$ species may be prepared and isolated by treatment of $(\text{TPP})_2\text{M}$ with phenoxathiinium hexachloroantimonate,¹² $(\text{C}_{12}\text{H}_8\text{SO})\text{SbCl}_6$, in CH_2Cl_2 . Crystallization from CH_2Cl_2 /toluene or CH_2Cl_2 /pentane yields $[(\text{TPP})_2\text{Th}][\text{SbCl}_6]$ ¹³ and $[(\text{TPP})_2\text{U}][\text{SbCl}_6]$ ¹⁴ as blue-violet crystalline solids. The Soret bands of these compounds appear at 396 and 392 nm, respectively, and are shifted to higher energy with respect to the neutral precursors (402 and 404 nm). The π -radical cation nature of $[(\text{TPP})_2\text{M}][\text{SbCl}_6]$ is supported by the presence of new bands in the IR spectra¹⁵ of the oxidized species at 1297 and 1264 cm⁻¹ for M = Th and at 1305, 1274, and 1266 cm⁻¹ for M = U. The $[(\text{TPP})_2\text{M}][\text{SbCl}_6]$ complexes are EPR active in frozen CH_2Cl_2 glasses at 77 K and exhibit signals at $g = 1.9985$ (line width 4.7 G) and $g = 1.9975$ (line width 5.9 G) for M = Th and U, respectively. In each case there is no observed anisotropy in the g -tensor under these experimental conditions.

$[(\text{TPP})_2\text{Th}][\text{SbCl}_6]$ is NMR silent in CH_2Cl_2 , but $[(\text{TPP})_2\text{U}][\text{SbCl}_6]$ is not (although the lines are broadened), which

(7) Deisenhofer, J.; Ep, O.; Miki, K.; Huber, R.; Michel, H. *J. Mol. Biol.* **1984**, *180*, 385–398.

(8) Davis, M. S.; Forman, A.; Hanson, L. K.; Thornber, J. P.; Fajer, J. *J. Phys. Chem.* **1979**, *83*, 3325–3332.

(9) Anal. Calcd for $(\text{TPP})_2\text{Th}$: C, 72.5; H, 3.88; N, 7.69; Th, 15.9. Found: C, 72.6; H, 3.81; N, 7.59; Th, 15.5. UV-vis (CHCl_3 , 25 °C) 402 nm (Soret); ¹H NMR (CDCl_3 , -40 °C) δ 9.33 (d, $J_{\text{HH}} = 7.4$ Hz, o-H), 8.34 (s, pyrrole-H), 8.0 (t, $J_{\text{HH}} = 7.6$ Hz, m-H), 7.75 (t, $J_{\text{HH}} = 7.6$ Hz, p-H), 7.23 (t, $J_{\text{HH}} = 7.6$ Hz, m-H), 6.56 (d, $J_{\text{HH}} = 7.5$ Hz, o-H); FDMS, m/e 1456 (M^+).

(10) Watt, G. W.; Gadd, K. F. *Inorg. Nucl. Chem. Lett.* **1973**, *9*, 203–205.

(11) Similar redox behavior has been noted for $(\text{TPP})_2\text{Ce}$, although the radical cations detected electrochemically have not been isolated: (a) Buchler, J. W.; De Cian, A.; Fischer, J.; Kihn-Botulinski, M.; Paulus, H.; Weiss, R. *J. Am. Chem. Soc.* **1986**, *108*, 3652–3659. (b) Buchler, J. W.; Elsässer, K.; Kihn-Botulinski, M.; Scharbert, B. *Angew. Chem., Int. Ed. Engl.* **1986**, *25*, 286.

(12) Gans, P.; Marchon, J.-C.; Reed, C. A.; Regnard, J.-R. *Now. J. Chim.* **1981**, *5*, 203–204.

(13) Anal. Calcd for $[(\text{TPP})_2\text{Th}][\text{SbCl}_6] \cdot 1/4\text{CH}_2\text{Cl}_2$: C, 58.5; H, 3.15; N, 6.18; Th, 12.8; Sb, 6.71; Cl, 12.7. Found: C, 58.3; H, 3.32; N, 5.83; Th, 12.9; Sb, 6.62; Cl, 12.8.

(14) Anal. Calcd for $[(\text{TPP})_2\text{U}][\text{SbCl}_6] \cdot 2\text{C}_2\text{H}_5 \cdot 2\text{CH}_2\text{Cl}_2$: C, 58.0; H, 3.7; N, 5.2; U, 11.1; Sb, 5.7; Cl, 16.5. Found: C, 58.7; H, 3.6; N, 4.9; U, 10.9; Sb, 5.7; Cl, 17.1. ¹H NMR (CD_2Cl_2 , -60 °C) δ 9.00 (d, $J_{\text{HH}} = 6.2$ Hz, o-H), 8.85 (s, fwhm = 18 Hz, m-H), 5.80 (t, $J_{\text{HH}} = 7.0$ Hz, p-H), 3.82 (s, fwhm = 27 Hz, m-H), 0.47 (s, fwhm = 30 Hz, o-H), -3.48 (s, fwhm = 29 Hz, pyrrole-H).

(15) Shimomura, E. T.; Phillippi, M. A.; Goff, H. M.; Scholz, W. F.; Reed, C. A. *J. Am. Chem. Soc.* **1981**, *103*, 6778–6780.